Egyptian Journal of Aquatic Biology & Fisheries
Zoology Department, Faculty of Science,
Ain Shams University, Cairo, Egypt.
ISSN 1110 - 6131
Vol. 28(6): 2229 - 2260 (2024)
www.ejabf.journals.ekb.eg

Monitoring Heat Wave Characteristics Depending on Surface Air Temperature Variability Along the Egyptian Mediterranean Coast

Mohamed Moustafa[1]*, Ahmed Abdelhamid[1], Ahmed Adel[1], Mohamed Elbessa[1, 2], Magdy Farag[1], Mohamed Shaltout[1]

[1]Oceanography Department, Faculty of Science, Alexandria University, Alexandria, Egypt
[2]College of Maritime Transport and Technology (CMTT), Arab Academy for Science, Technology and Maritime Transport (AASTMT), Abu-Qir, Alexandria, Egypt

***Corresponding Author: Mohamed.mostafa_pg@alexu.edu.eg**

ARTICLE INFO

Article History:
Received: Nov. 19, 2024
Accepted: Dec. 25, 2024
Online: Dec. 28, 2024

Keywords:
Egyptian Mediterranean Coast,
Surface air temperature,
Heat waves,
ERA5

ABSTRACT

Due to its high population density, rapid urbanization, and vulnerability to climate change, Egypt faces significant climate-related risks, particularly along its coasts. The Egyptian Mediterranean Coast (EMC) has been identified as a "hot spot" for climate change, expected to experience increased surface air temperatures and more frequent, intense heatwaves, especially in the summer. Understanding the characteristics, trends, and impacts of heatwaves along the EMC is crucial for developing effective adaptation and mitigation strategies. This study utilized observational data (2007-2023) and ERA5 reanalysis data (1979-2023) to examine surface air temperature (T2m) across five key locations along the EMC: Marsa Matrouh, Ras El-Tin, Abu Qir, Port Said, and El Arish. The study aimed to: (1) analyze short-term fluctuations in T2m, (2) validate the accuracy of ERA5 in representing T2m, (3) apply bias correction to ERA5 data, and (4) assess the frequency, intensity, duration, and timing of heatwaves. The results showed a positive temperature monotonic trend over the past decades, with significant increases in heatwave frequency and duration. Port Said and El Arish exhibited the most pronounced warming trends and heatwave intensification. The study underscores the urgent need for climate adaptation strategies to address the growing risks of heatwaves in this vulnerable coastal region.

INTRODUCTION

Egypt is often identified as a vulnerable country to various environmental and socio-economic challenges. The country faces significant risks from climate change, particularly due to its geographical features and population distribution. Egypt experiences extreme temperatures, dust storms, and flash floods, which can have severe impacts on infrastructure, agriculture, and human health. Efforts are being made to address these vulnerabilities through various adaptation and mitigation strategies, but the challenges remain significant.

As global temperatures rise, Egypt, with its arid and semiarid regions, will suffer from:

- Agricultural stress: Higher temperatures and reduced water availability can stress agricultural systems, leading to lower crop yields and increased water demand for irrigation **(Mostafa *et al*., 2021)**.

- Increased evaporation: Higher temperatures lead to increased evaporation rates, reducing the overall availability of surface water.

- Reduced Nile flow: Climate change impacts on the Nile River, Egypt's primary water source, could lead to reduced flow and availability.

- Groundwater depletion: Over-reliance on groundwater due to surface water scarcity can lead to depletion and deterioration of groundwater quality **(Gado & El-Agha, 2021)**.

The Egyptian Mediterranean coast (EMC), which extends from 27°E to 33° is considered an arid zone except for El Arish, which is considered a semi-arid zone **(UNESCO, 1979)**. According to **UNESCO (1979)**, the aridity index, defined as the ratio of annual precipitation to potential evapotranspiration, ranges from 0.03 to 0.2 at the arid zone and from 0.2 to 0.5 at the semi-arid zone. Additionally, the EMC has been identified as a climatic "hot spot," expected to experience notable changes, including an increase in surface air temperatures (positive trend), a decrease in precipitation (negative trend), and a minor decline in sea level pressure by the end of the 21st century as stated by **(Shaltout *et al*., 2013; IPCC, 2019; Tuel & El Tahir, 2020)**. **Gentilucci *et al*. (2021)** mentioned that the EMC expected to experience increased surface air temperatures and more frequent and intense heatwaves, especially during summer. Also, it experiences a wide range of temperature throughout the year, which is influenced by both seasonal changes and climatic patterns.

The EMC climate describes seasonal variation. During the summer season (June, July, and August), the Indian Summer Monsoon (ISM) affects the atmospheric circulation patterns, which can extend their influence on the eastern Mediterranean region. Additionally, the Azores High, a semi-permanent high-pressure system in the North Atlantic, plays a crucial role in the summer climate of the EMC. It influences prevailing wind patterns and can lead to stable, dry conditions along the coast **(Yadav, 2021; Eldeeb & Elemam, 2022)**.

The Azores High, linked to a mild climate, extends eastward, while the ISM, associated with a thermal low, expands northwest. During the summer months, when the ISM dominates over the EMC, there is a significant rise in temperature and dry conditions. In contrast, when the Azores High prevails over the southeastern Mediterranean, it tends to moderate both temperature and dryness **(Elbessa & Shaltout, 2024)**. The air temperature in the eastern Mediterranean region is indeed influenced by large-scale climate oscillations like the North Atlantic Oscillation (NAO). These oscillations can cause significant inter-annual variability in temperature patterns.

During the positive phase, the eastern Mediterranean typically experiences warmer and wetter conditions. This is due to stronger westerly winds that bring warm, moist air from the Atlantic into the region. In the negative phase, the region tends to have cooler and drier conditions. This is because the westerly winds weaken, allowing colder air from the north to penetrate further south **(Clark & Feldstein, 2020)**.

Sometimes, when a high-pressure area moves from the United Kingdom towards Scandinavia, it tends to strengthen. This is associated with the formation of a Blocking Anticyclone, commonly referred to as the omega block, which inhibits the normal eastward progression of Mediterranean depressions. This blocking pattern results in calm, dry weather across central-western Europe, while the central-eastern regions of Europe and the eastern Mediterranean, including northern Egypt, experience colder conditions. As the omega block moves over the Mediterranean Sea, it gathers moisture, leading to increased rainfall in North Africa. Additionally, when an omega block coincides with the presence of the Siberian High, a notable drop in temperatures and an increase in snowfall are observed in parts of North Asia and northeastern Africa **(Kautz *et al.*, 2022)**.

Specifically, **De Vries *et al.* (2013)** showed that the Siberian High system significantly influences climate/weather fluctuations over the EMC and its surrounding continent. The Siberian High system, which is responsible for polar outbreaks over the Mediterranean Sea **(Saaroni *et al.*, 1996)**, tends to increase the likelihood of the rainy season developing, which, when combined with the Mediterranean low-pressure system, generates easterly storms over the EMC **(Saaroni *et al.*, 1998; Nastos & Zerefos, 2009)**. The southward movement of the Siberian High and Azores High over the Mediterranean Sea produces numerous advantages for precipitation and the development of extratropical storms **(Haggag & El-Badry, 2013)**. Furthermore, when the Azores High (winter subtropical high-pressure systems) move southward, storm systems from the Atlantic Ocean tend to penetrate the Mediterranean Sea **(Zerefos *et al.*, 2011)**. Moreover, severe weather occurrences over the EMC during the winter season are strongly linked to Mediterranean cyclones and very rarely occur under other conditions **(Lionello *et al.*, 2006)**.

Given the critical importance of heatwaves to the EMC's climate resilience, understanding their characteristics, future trends, and impacts is essential for effective adaptation and mitigation strategies, where heatwaves are defined as prolonged periods of excessively high temperatures that significantly exceed the average for a particular region, often leading to adverse impacts on human health, ecosystems, and the economy **(Lelieveld *et al.*, 2016)**. Recently the Mediterranean region, including Egypt, has seen an increasing frequency and intensity of such heat events, especially during the summer months **(Tonbol *et al.*, 2018)**.

Heatwaves over the EMC are typically driven by a combination of factors, including atmospheric blocking patterns, the influence of the subtropical high-pressure systems (such as the Azores High), and the interaction with warm, dry air masses originating from the Sahara Desert **(Alpert *et al.*, 2008; Shaltout *et al.*, 2013)**. During

the summer, when the Azores High strengthens and expands over the region, temperatures in coastal cities such as Alexandria, Marsa Matrouh, and Port Said can rise sharply, with maximum temperatures often exceeding 40°C **(El-Geziry *et al.*, 2021)**. These heat events are exacerbated by the urban heat island effect in major cities, where high population density, unplanned urbanization, and limited green spaces contribute to elevated temperatures **(Domroes & El-Tantawi, 2005)**.

Moreover, the frequency of heatwaves over the EMC is expected to increase significantly under future climate change scenarios. Climate models, such as those using the RCP4.5 and RCP8.5 pathways, indicate that by the end of the century, the region may experience increases in surface temperatures ranging from 0.6 to 2.8°C **(Shaltout *et al.*, 2013; IPCC, 2014)**. These temperature increases are likely to result in more frequent, prolonged, and intense heatwaves, with potential impacts on public health, agriculture, and energy consumption **(Bucchignani *et al.*, 2018)**. The increased frequency of heatwaves is also associated with changes in precipitation patterns, with a tendency toward more prolonged dry periods and reduced rainfall, which further compounds the risk of droughts and desertification in the region **(Lelieveld *et al.*, 2016; Tonbol *et al.*, 2018)**.

The vulnerability of the EMC to heatwaves is of particular concern given its dense population and critical infrastructure. Cities such as Alexandria and Port Said, which are situated along the coast, are exposed to both the urban heat island effect and rising temperatures due to their coastal locations **(Mahfouz *et al.*, 2020)**. In addition, the economic activities along the EMC, including agriculture, fishing, and tourism, are highly sensitive to extreme heat events, as heatwaves can reduce productivity, disrupt food supplies, and deter tourists **(Alcamo *et al.*, 2007)**. Furthermore, increasing sea surface temperatures, linked to the intensification of heatwaves, may also lead to rising humidity levels, which amplify the heat stress experienced by vulnerable populations **(Alpert *et al.*, 2008)**.

Earlier studies in marine heatwaves are available offering insightful information and fundamental understanding. **Ibrahim *et al.* (2021)** mentioned that marine heatwaves (MHWs) can cause devastating impacts on marine life, the frequency of MHWs is expected to rise significantly as the climate continues to warm. MHWs intensity and count are pronounced with many parts of the oceans and semi enclosed seas, such as Eastern Mediterranean Sea (EMED). Over the period 1982-2020 there was a clear decadal increase in MHWs frequency in all EMED locations with a significantly positive frequency trend of 1.2 events per decade, where the mean MHW frequency and duration increased by 40 and 15%, respectively, and the average MHW cumulative intensity trend increased by 5.4°C/ days. Atmospheric conditions, such as mean sea level pressure, wind stress, and air temperature, could be related to the occurrence of marine heatwaves (MHWs). For instance, high air temperatures (>25°C) have been linked to the locations of extreme MHW events. In the same context **Aboelkhair *et al.* (2023)** revealed that there was a high statistically significant correlation between atmospheric heatwaves and

marine heatwaves, where during the period of 1982-2021, more than half of the marine heatwaves in the EMED co-occurred with atmospheric heatwaves.

Marine heatwaves could increase the social, economic, and environmental impacts of climate change in the Mediterranean region especially due to its high population. MHWs have progressively become more frequent and intense and have a larger duration in the Mediterranean region with a clear acceleration of this trend since 2000, especially in the last decade. The growing trend of MHWs will increase their impact on marine life and is also likely to trigger heavy precipitation events in the Mediterranean Basin, due to their effect on heat and moisture exchanges at the air-sea interface **(Pastor & Khodayar, 2023)**.

Previous research on surface air temperature based on data from 1971 to 2000 indicated that in Marsa Matrouh the annual average temperature was 19.5°C, with a warming trend of 0.18°C per decade, in Alexandria the annual average temperature was 20.3°C, with a warming trend of 0.1°C per decade, in Port Said the annual average temperature of 20.3°C with a slight cooling trend of -0.06°C per decade **(Domroes & El-Tantawi, 2005)**. Using the ERA-Interim dataset (1979-2010), **Shaltout *et al*. (2013)** found the annual average temperature in Marsa Matrouh ranged from 20 to 20.5°C, with a warming trend of 0.4-0.5°C per decade, in Alexandria the annual temperature ranged from 20 to 20.5°C with a warming trend of 0.3-0.4°C per decade, in Port Said the daily temperatures ranged between 7 and 34°C, with an annual mean of 21.2°C. Moreover, in El Arish, the annual average temperature was 20.5°C with a warming trend of 0.5-0.6°C per decade. From 2007 to 2018, the monthly temperatures in Marsa Matrouh fluctuated from 12.26°C in January to 27.93°C in August, with an annual warming trend of 0.45°C per decade, in Alexandria monthly temperatures showed significant variation, reaching a peak of 29°C in August and a minimum of 14°C in January, with a warming trend of 0.2-0.5°C per decade, in Port Said monthly temperatures ranged between 13.61°C in January and 29.50°C in August, In El Arish hourly temperatures showed significant variation, peaking at 29.3°C in August and dropping to 12°C in January, with a warming trend of 0.57°C per decade and an annual average of 21.55°C **(Tonbol *et al*., 2018)**. During the period 2007-2019, hourly temperatures in Marsa Matrouh varied between a minimum of 5.2°C and a maximum of 43.4°C, with an annual average of 20.6°C, in Alexandria the hourly temperatures varied from 5.2 to 41.0°C, with an annual average of 21.9°C. Furthermore, in El Arish the hourly temperatures ranged between 2.0 and 45°C, with an average of 21.6°C **(El-Geziry *et al*., 2021)**. **Mahfouz *et al*. (2020)** reported that hourly temperatures from 2007 to 2018 in Alexandria ranged between 7 and 41°C, with a warming trend of 0.3-0.4°C per decade.

Looking forward, **Alcamo *et al*. (2007)** projected that temperatures in the northern Mediterranean under the A1B scenario will experience a warming trend of 0.22-0.5°C per decade until 2100. **Alpert *et al.* (2008)** predicted a temperature increase of 3 to 4°C per decade in the Eastern Mediterranean under the A2 and B2 scenarios, comparing the periods 2071-2100 and 1961-1990. The EMC is expected to undergo significant warming

by the end of the century, with temperature increases ranging from 0.6 to 2.8°C relative to the 1981-2010 average, according to **Shaltout *et al*. (2013)**. Future warming trends in the EMC are expected to range from 0.6 to 2.6°C, depending on the scenario used. Overall, future warming patterns over the study area are consistent across regional and global climate models under the A1B and A2 scenarios **(IPCC, 2014)**. Additionally, **Lelieveld *et al*. (2016)** confirmed a notable warming trend, especially in summer, across the MENA region using the ensemble results from CMIP5 models under the RCP4.5 and RCP8.5 scenarios. **Bucchignani *et al*. (2018)** projected a significant warming trend in the Middle East-North Africa region, ranging from 2.5 to 4°C per decade under the RCP4.5 scenario, using the COSMO-CLM regional climate model.

2- USED DATA AND METHODS OF ANALYSIS

1. The framework of this study aimed to:

- Utilize the observed data to depict the existing short and/long-term fluctuations in air surface temperature (T2m) from 2007 to 2023.
- Validate ERA5 accuracy in representing T2m.
- Apply the cumulative distribution function (CDF) of the observed data with the CDF of the ERA5 for bias correction to ERA5 data (1979-2023).
- Assess heatwave frequency, intensity, duration, and timing.

2. Required data

To analyze the surface air temperature distribution and its impacts, the present study focused on:

2.1 Five automated weather observation systems (AWOS):

Five key locations at the EMC were selected to represent a range of climatic conditions and geographical features typical of the EMC.

- Five AWOS along the EMC were used to collect T2m at Marsa Matrouh, Ras El-Tin, Abu Qir, Port Said and El Arish, as shown in Table (1).
- These five AWOS were installed and maintained according to World Meteorological Organization (WMO) regulations, where T2m is calibrated to WMO standard height of 2m.
- These T2m measurements are well-distributed spatially along the EMC and were collected on an hourly basis from 2007 to 2023. The average percentage of missing data across all stations during the study period ranges from 0.06% to 0.17%, which is considered negligible. This percentage includes only the hourly data points with no missing values in both the observed dataset and the ERA5 reanalysis.

Table 1. Elevations and positions of Meteorological working stations

Station Names	IN	Height above sea level (m)	Geographic Position		International Station NO.
			Latitude (N)	Longitude (E)	
Marsa Matrouh	1	20	31° 21` 34``	27° 14` 43``	62304
Ras El-Tin	2	21.95	31° 11` 50``	29° 51` 49``	62317
Abu Qir	3	26.6	31° 19` 55``	30° 5` 6``	62320
Port Said	4	19.75	31° 15` 19``	32° 18` 17``	62334
El Arish	5	15	31° 08` 54``	33° 49` 27``	62331

2.2 ERA5 database

The ERA5 database, distributed by the Copernicus Climate Change Service (C3S) and produced by the European Centre for Medium-Range Weather Forecasts (ECMWF), was designed to build upon the successes of previous datasets such as ERA-Interim and ERA40. Its goal is to improve atmospheric parameter estimates **(Hersbach *et al.*, 2020)** with a finer spatial resolution of 0.25° x 0.25° (MATLAB code was used to downscale the data from a grid to individual points) and an hourly temporal resolution.

After validating the data with observations, they were used to analyze long-term trends in the studied atmospheric variables. Additionally, these data were used to statistically downscale global climate simulations for the five studied stations.

2.3 Data requirements

The data used in this study were obtained from the two different sources as follows:

- Hourly observed air temperature (T2m) from the five Egyptian weather stations between 2007 and 2023.
- ERA5 hourly estimated air temperature at these five stations.
- Hourly data from 1979 to 2023 were freely obtained from the European Eyes on Earth (Copernicus) website: https://cds.climate.copernicus.eu/cdsapp#!/dataset/reanalysis-era5-single-levels?tab=form.

Direct comparisons of the hourly observed data and ERA5 were conducted to assess the efficiency of ERA5 at the five studied stations.

3. Methods of analysis

3.1 Statistical analysis

3.1.1 Data evaluation

- The f- and t-tests were used to examine whether ERA5 and the observations can display the means and variances of equal populations or not at a 95% significance level, and
- ERA5 databases were subjected to CDF bias correction depending on observed used data (from 2007 to 2023), whilst the years from 2021 to 2023 were used for the validation processes between ERA5 and observation.

3.1.2 Primary statistical analysis

- The surface observed data (T2m, 2007–2023) were subjected to primary statistical analysis, including minimum, mean, maximum, and standard deviation.
- Anomaly detection: Comparisons between the different temperature datasets and a baseline period will be made to identify deviations or anomalies.

3.1.3 Advanced statistical analysis

- Cumulative distribution function (CDF) was used to provide a more detailed view of the temperature distribution, which is useful for bias correction.
- Frequency distributions for different temporal scales (daily, monthly, and annual) across the five weather stations were analyzed to understand and identify trends, patterns, and anomalies.
- Linear regression analysis was applied to: a. Understand climate variability and predict future trends. b. Identify and assess long-term temperature changes. c. Assess the impact of climate change.

3.2 ERA5 efficiency test, bias removal, and trend analysis

Direct comparisons between the hourly observed data and ERA5 were used to test the efficiency of ERA5 at the five stations studied. Additionally, f- and t-tests were employed to examine whether ERA5 and the observations display equal means and variances (i.e., whether they come from the same population) at a 95% significance level. Furthermore, the ERA5 data underwent CDF bias correction based on the comparison between ERA5 and observed data for the calibration period (2007–2020), while the years 2021–2023 were used for validation between ERA5 and the observations.

According to **Vigaud *et al*. (2013)**, the CDF approach can be used as follows:

$$T\left(E_h(x)\right) = \left(F_h\left(x\right)\right) \qquad [1]$$

Where, F_h represent the CDF of observed local data from 2007 to 2020; E_h represent the CDF of ERA5 outputs bi-linearly interpolated at the exact station location. Based on the presumption that a transformation T exists, transforming ERA5 variable (predictor) into the CDF representing the observation (predictand) at the specified weather station, the bias correction implemented T: [0, 1] → [0, 1].

Replacing x by E_h^{-1} (u) in equation (1) with $u \in$ [0, 1] allows the following definition for the transform T:

$$T\left(u\right) = F_h(E_h^{-1}\left(u\right)) \qquad [2]$$

The present strategy for bias correction is to match the CDF of the observations to the CDF of the ERA5 database at the station level. The spatial mismatch between the point observation and the ERA5 grid cell is a challenge in this bias correction. Only stationary points were analyzed in the current study. Therefore, our strategy made use of this bias correction. Moreover, the technique of calibration and validation was used to test the efficiency of ERA5 to describe the air temperature over the studied five stations. This strategy was used by many researchers. **Anagnostou *et al*. (1999)** used the CDF strategy to statistically adjust the satellite microwave for monthly rainfall estimates. Furthermore, **Wood *et al*. (2002)** used the CDF technique for long-range hydrologic forecasting.

Reichle and Koster (2004) used this strategy to match the CDF between satellite retrievals and model soil moisture. Finally, **Bawadekji *et al*. (2022)** used this strategy to match the CDF between observed and ERA5 atmospheric parameters along the Red Sea Saudi Arabia coast.

A linear trend analysis, based on the ERA5 after correction (hereafter, C_ERA5) from 1979 to 2023, was used to characterize the current long-term surface air temperature along EMC over the studied five stations. Moreover, the non-parametric Mann-Kendall test **(Mann, 1945; Kendall, 1975)** was used to detect monotonic trends in C_ERA5 to examine whether C_ERA5 follows a significant (monotonic) trend or not **(Elbessa *et al.*, 2021)**. The limitations of the Mann-Kendall test are frequently associated with data that has serial correlation. The term "serial correlation" refers to the relationship between two variables with various lag periods. Each observation is independent of the other if the serial correlation of a variable is 0. If the serial correlations tend to be one, the observations are serially correlated, and the Mann-Kendall test will not identify monotonic trends, to avoid this limitation in the studied atmospheric parameters, the trend-free pre-whitening technique was used **(Wang *et al*., 2020)**.

In addition, the studied atmospheric parameter was analyzed to establish the dates of the historically most extreme events (date of the maximum/minimum values) based on the C_ERA5 hourly data.

3.3 Heatwaves characteristics

The World Meteorological Organization notes that there is no universally accepted definition of heatwaves. In literature, several definitions, indices, and measures are used by meteorological agencies and other authorities. Some definitions are based on regional norms or fixed temperature thresholds, while others employ percentage-based criteria. In this study, a heatwave is defined as an event that lasts for at least two days or more where both minimum and maximum daily temperatures exceed the 85^{th}, 90^{th}, 95^{th}, and 99^{th} percentiles of historical daily temperature records. These categories are labeled as mild, moderate, severe, and extreme heatwaves, respectively, which are commonly used in heatwave research **(Shafiei *et al.*, 2019)**.

In this study, we will focus on the following specific heatwave components for each station using MATLAB and R Studio software to analyze the available meteorological data:

- Number of hot days (Days): Days in which both the maximum and minimum temperatures exceed predefined thresholds.
- Heatwave frequency: The number of distinct heatwave events occurring within a given year.
- Heatwave duration: The cumulative length of all heatwaves experienced during a year.

- Heatwave intensity: The average severity of heatwaves, defined as the sum of temperatures above the predefined maximum and minimum thresholds during both daytime and nighttime.
- Heatwave appearance period: The period marking the onset and end of heatwaves over the years.

RESULTS AND DISCUSSION

1. Observed data

Table (2) shows the average of the annual, monthly, and hourly characteristics for T2m based on observed data during the period 2007-2023 overall studied stations. The scatter plot (Cluster) interpretations are shown in Fig. (1):

- The Hourly: average maximum temperatures in the range of 23-25°C and minimum temperatures around 16-19°C.
- The Monthly: the average monthly data, with maximum temperatures around 27-29°C and minimum temperatures between 15-17°C.
- The Annual: showing lower maximum temperatures average around 22-24°C and minimum temperatures between 20-21°C.

Generally, the scatter plot shows the proximity of the Ras El-Tin and Abu Qir stations, which are grouped closely together, while the other stations are more spread out, particularly El Arish and Marsa Matrouh stations. This pattern can be explained by the geographical differences between these stations. El Arish and Marsa Matrouh are in desert areas, which may lead to more variable temperature ranges due to the dry nature of the land. In contrast, Ras El-Tin, Abu Qir, and the other stations are in delta regions, where proximity to the coast results in more moderate temperature variations. This difference in terrain likely influences the temperature patterns recorded at each station.

Table 2. Annual, monthly, and hourly characteristics for T2m based on hourly Observed data during the period 2007 to 2023 over Marsa Matrouh, Ras El-Tin, Abu Qir, Port Said and El Arish.

Station		Marsa Matrouh	Ras El-Tin	Abu Qir	Port Said	El Arish
Annual	Max	2010	2018	2010	2010	2010
		21.56°C	22.38°C	22.26°C	22.90°C	22.31°C
	Min	2011	2022	2011	2007	2007
		19.64°C	21.25°C	21.16°C	21.68°C	21.00°C
Monthly	Max	August	August	August	August	August
		26.96°C	27.69°C	27.99°C	28.56°C	28.40°C
	Min	January	January	January	January	January
		14.05°C	15.43°C	15.67°C	15.02°C	14.04°C
Hourly	Max	At 1300	At 1300	At 1300	At 1300	At 1200
		23.27°C	23.02°C	23.63°C	24.64°C	25.09°C
	Min	At 0500	At 0400	At 0400	At 0400	At 0400
		17.80°C	20.09°C	20.24°C	19.94°C	18.26°C

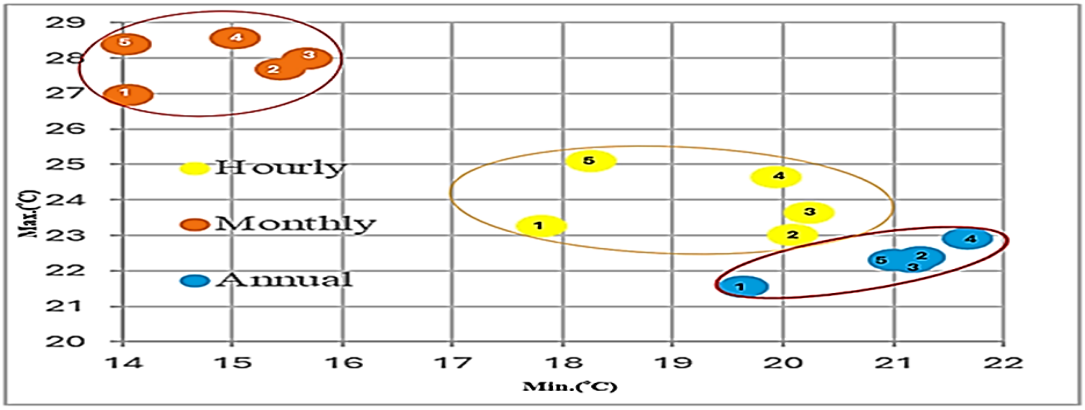

Fig. 1. A scatter plot of maximum and minimum temperatures classified by different time resolutions: hourly (yellow), monthly (orange), and annual (blue). Each data point, numbered from 1 to 5, represents five weather stations: 1) Marsa Matrouh, 2) Ras El-Tin, 3) Abu Qir, 4) Port Said, and 5) El Arish.

1.1 Monthly average time series

The monthly average time series for T2m, based on hourly observed data from 2007 to 2023, for Marsa Matrouh, Ras El-Tin, Abu Qir, Port Said, and El Arish, revealed that January 2012 was the coldest month during the study period at Marsa Matrouh and Abu Qir, with temperatures of 12.26 and 14.02°C, respectively. In contrast, January 2022 was the coldest month at Ras El-Tin and Port Said, with temperatures of 14.17 and 13.46°C, respectively. At El Arish, January 2008 recorded the lowest temperature, with a value of 12.02°C. On the other hand, August 2015 was the warmest month during the study period at all five stations, with temperatures of 27.93°C at Marsa Matrouh, 29.08°C at Ras El-Tin, 28.55°C at Abu Qir, 29.50°C at Port Said, and 29.31°C at El Arish.

1.2 Annual time series

Annual average time series for T2m based on hourly observed data from 2007-2023 over Marsa Matrouh, Ras El-Tin, Abu Qir, Port Said and El Arish are shown in Fig. (2), where T2m data analysis revealed that 2010 was the hottest year during the study period at Marsa Matrouh, Ras El-Tin, Port Said and El Arish with a value of 21.56, 22.26, 22.90, and 22.31°C, respectively. While at Abu Qir, the hottest year during the study period was 2018 with a value of 22.38°C. Otherwise, T2m annual average reached its minimum at Marsa Matrouh, and Ras El-Tin in 2011 with a value of 19.64 and 21.17°C, respectively. Otherwise, at Port Said and El Arish the minimum T2m annual average was in 2007 with a value of 21.68 and 21.00°C, respectively. While at Abu Qir, the minimum T2m annual average was in 2022 with a value of 21.25°C.

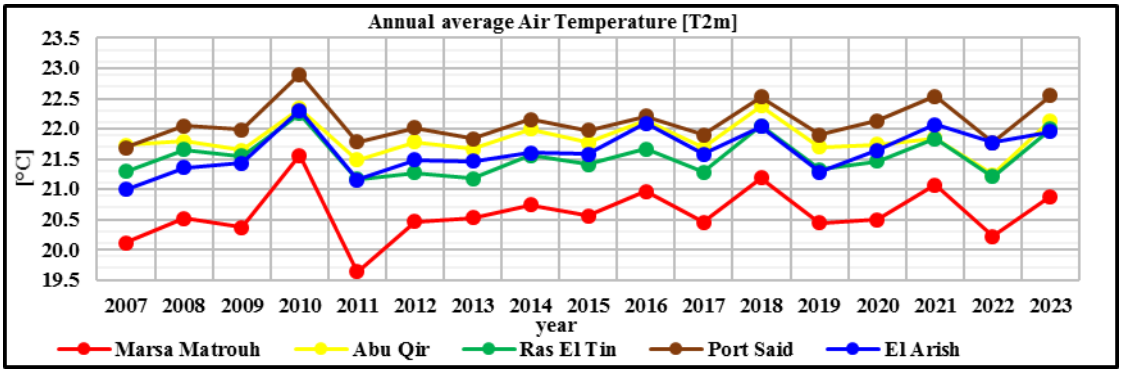

Fig. 2. Annual average time series for T2m based on hourly Observed data (2007-2023) over Marsa Matrouh, Ras El-Tin, Abu Qir, Port Said and El Arish

1.3. Annual and daily temperature cycle

The annual cycle (Multi-year Monthly average) of surface air temperature is described in Table (2) and Fig. (3). The annual T2m cycle has a maximum value in August and a minimum value in January along the studied five stations. The amplitude of the T2m annual cycle describes a variation (MAX T2m - MIN T2m) from 12.25°C at Ras El-Tin to 14.37°C at El Arish.

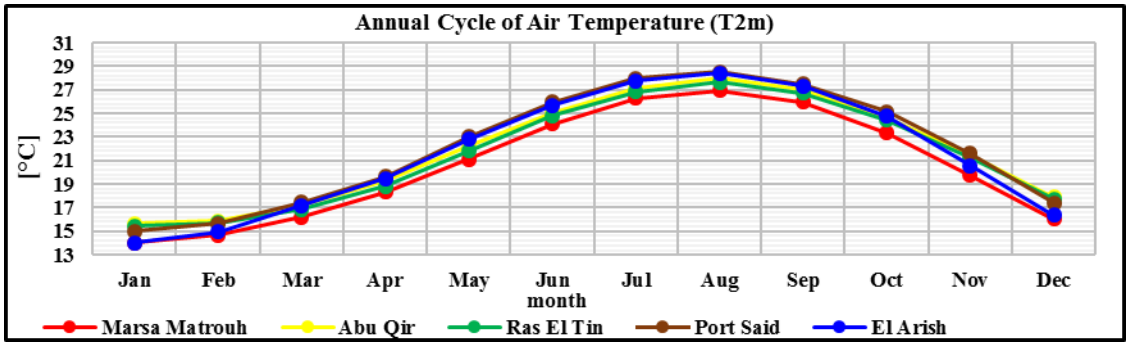

Fig. 3. Short-term monthly means (Annual cycle) for T2m based on hourly observed data (2007 - 2023)

The daily cycle (Multi-year hourly average) of surface air temperature is described in Table (2) and Fig. (4). The amplitude of the daily T2m cycle over El Arish (6.83°C) was much higher than that of Marsa Matrouh (5.47°C), Port Said (4.69°C), Abu Qir (3.39°C), and Ras El-Tin (2.93°C). In detail, the T2m showed a diurnal cycle along EMC whereas the minimum value occurred between 0400-0500 and the maximum values occurred between 1200-1300. T2m daily range showed its maximum value over El Arish and its minimum value over Ras El-Tin.

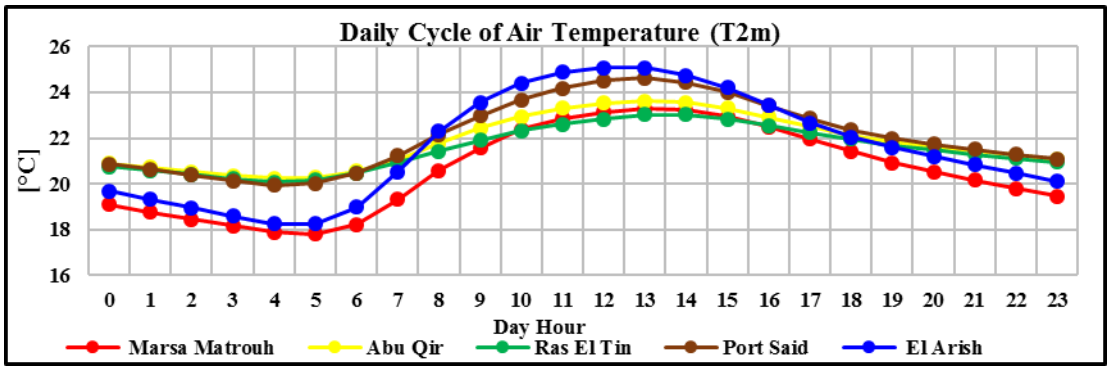

Fig. 4. Observed short-term hourly means (Daily cycle) for the parameters under study based on hourly observed data (2007- 2023)

2. ERA5 reanalysis data

2.1 ERA5 Calibration

To evaluate the conveniently of using ERA5 in describing T2m over Marsa Matrouh, Ras El-Tin, Abu Qir, Port Said and El Arish, a comparison was carried out between observations data and ERA5 datasets covering the observation period from 2007 to 2023, where results are represented in Table (3). In general, ERA5 reanalysis data have closely matched the observations over the five stations studied. ERA5 lower estimate T2m observation at Ras El-Tin, Abu Qir, Port Said and El Arish by 0.64, 0.43, 0.49, 0.4°C, respectively. In contrast, they are showing an overestimate at Marsa Matrouh by 0.12°C. In the same context, analyses of the skewness coefficient showed that ERA5 reanalysis data and observed T2m have an almost symmetrical distribution with a small tendency towards negative skewness over the five studied stations.

At a 99% significance level, statistical tests (t- and f-tests) indicated that ERA5 and observed datasets of T2m values come from two equal distributions of mean and variance.

Table 3. Comparison analysis (hourly/annually) between observed and ERA5 T2m over studied stations. (Obs = Observed, n = number of observations, R = correlation coefficient in percentage, Skw=Skewness, Med.=Median , Min = minimum, Max = Maximum, and St. dv = Standard Deviation)

Variables			n	R [%]	hourly				Annual	
					Skw	Med.	Min.	Max.	Med.	Annual mean ± St. dev of the annual cycle
Surface air temperature (T2M, °C)	Marsa Matrouh	Obs.	148854	0.96	-0.09	20.80	5.20	43.40	20.52	20.60±5.38
		ERA5			0.03	20.85	5.05	44.20	20.67	20.72±5.87
	Ras El-Tin	Obs.	148824	0.98	-0.09	22.00	1.7	41	21.78	21.83±4.88
		ERA5			-0.08	21.20	8.2	35.88	21.10	21.18±4.51
	Abu Qir	Obs.	148758	0.97	-0.13	21.80	1.00	38.00	21.47	21.54±4.79
		ERA5			-0.09	21.30	7.00	36.70	21.02	21.11±4.75
	Port Said	Obs.	148920	0.98	-0.17	22.50	2.40	40.70	22.01	22.11±5.38
		ERA5			-0.16	21.90	7.60	37.60	21.56	21.62±4.86
	El Arish	Obs.	148920	0.96	-0.19	22.00	1.00	45.00	21.59	21.64±5.95
		ERA5			-0.15	21.50	6.90	36.60	21.12	21.24±4.97

Notes: The comparison analysis between observed T2m and ERA5 data at the stations studied was performed on an hourly basis. The minimum and maximum values occurred rarely during the study period and were associated with southern wind direction from land during the summer season. This will be considered in future studies as a case study

2.2 ERA5 bias correction

To remove ERA5 bias, CDF bias correction was applied to match the CDF of the ERA5 to the CDF of the observation from 2007 to 2023, as seen in Fig. (5). This technique preserves the nature of the data by adjusting the bias to zero and saves the correlation values as the same values. This strategy was applied for the long-term ERA5 database to calculate the corrected ERA5 reanalysis data (C_ERA5) over the five studied stations. Fig. (5) proves the current results that ERA5 reanalysis data more reasonably simulates T2m over all stations as the three curves of observations, ERA5, and C_ERA5 are so close.

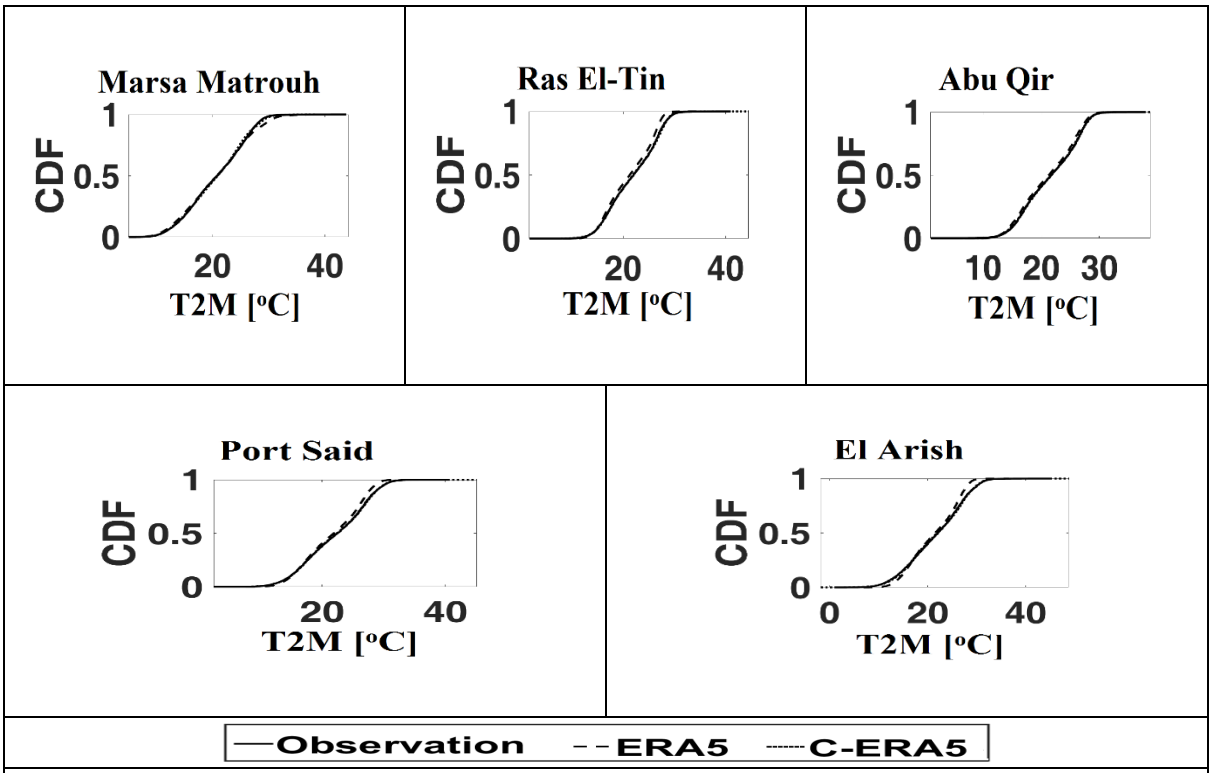

Fig. 5. Matching the CDF of T2m ERA5 to the CDF of T2m observation from 2007 to 2023

2.3 ERA5 validation

In this section, the validation was used to evaluate whether a calculated statistical model during the calibration period is appropriate or not. Table (4) shows the comparison between ERA5 and C_ERA5 in describing T2m over the studied five stations. The C_ERA5 showed a lower bias with the observation than ERA5 did. However, the correlation between the C_ERA5 and observation showed a similar value as ERA5 did. Therefore, using C_ERA5 is useful and valid to describe the long-term current weather characteristics and gives a better weather description of the studied stations.

Table 4. The comparison between ERA5 and C_ERA5 in describing the weather characteristics over the studied five stations for the validation period (2007-2023).

Variables	Stations	Validation	r [%]	bias
Surface air temperature (T2M, °C)	Marsa Matrouh	Observed, ERA5	0.960	0.113
		Observed, Corr_ERA5	0.961	**0.000**
	Ras El-Tin	Observed, ERA5	0.977	0.644
		Observed, Corr_ERA5	0.976	**0.000**
	Abu Qir	Observed, ERA5	0.973	0.426
		Observed, Corr_ERA5	0.973	**0.000**
	Port Said	Observed, ERA5	0.979	0.492
		Observed, Corr_ERA5	0.978	**0.000**
	El Arish	Observed, ERA5	0.959	0.395
		Observed, Corr_ERA5	0.959	**0.000**

2.4 Corrected ERA5 statistical analysis

2.4.1 Annual trend analysis

C_ERA5 datasets (1979-2023) demonstrate that the annual average of T2m over the studied stations revealed a significant spatial variation as noticed in Table (5). In the same context, the T2m experienced a positive monotonic trend over the five studied stations. In detail for the period from 1979 to 2023, the warming trend along the study area showed a spatial variation with a positive trend over the EMC ranging from 0.03˚C at Marsa Matrouh, 0.04˚C at Ras El-Tin and Abu Qir, 0.05˚C at Port Said, and 0.06˚C at El Arish, as seen in Table (5).

Table 5. Long-term annual mean and trend analysis for corrected ERA5 T2m over studied stations from 1979 to 2023. The non-parametric (Mann-Kendall test) is used to detect monotonic trends in Corrected ERA5 to examine whether or not C_ERA5 follows a significant (monotonic) trend

Variables		Annual mean ± standard deviation	Trend (decade-1)	Significant (monotonic) trend
Surface air temperature (T2M, °C)	Marsa Matrouh	20.19 ± 5.4	0.03°C	Yes
	Ras El-Tin	21.25 ± 4.8	0.04°C	Yes
	Abu Qir	21.00 ± 4.8	0.04°C	Yes
	Port Said	21.40 ± 5.3	0.05°C	Yes
	El Arish	20.89 ± 5.9	0.06°C	Yes

2.4.2 Historical days

The T2m dataset during the study period revealed that the highest temperature recorded in the study area occurred on 22nd April 2008 at 1000 over Marsa Matrouh (35.8°C), on 8th May 2021 at 1600 over Ras El-Tin (44.5°C), on 30th May 2014 at 1500 over Abu Qir (38.8°C), on 4th June 2014 at 1500 over Port Said (45.2°C), and on 23rd May 2019 at 1400 over El Arish (48.8°C). Conversely, the lowest temperature occurred

on 18th February 2008 at 0600 over Marsa Matrouh (6.8°C), on 13th December 2013 at 0500 over Ras El-Tin (3.9°C), on 13th December 2013 at 0500 over Abu Qir (5.5°C), on 13th December 2013 at 0600 over Port Said (3.7°C), and on 15th January 2008 at 0600 over El Arish (-1.8°C).

2.4.4 The probability of occurrence

The highest occurrence percentage of hourly T2m was 7.06% (23-24°C), 8.44% (25-26°C), 8.31% (25-26°C), 7.52% (26-27°C), and 6.77% (26-27°C) over Marsa Matrouh, Ras El-Tin, Abu Qir, Port Said and El Arish, respectively. The percentage of occurrences during the hottest hours (mean+2*standard deviation) was 0.59% (>31.34°C), 0.20% (>31.59°C), 0.20% (>31.12°C), 0.16% (>32.87°C), and 0.24% (>33.52°C) over Marsa Matrouh, Ras El-Tin, Abu Qir, Port Said and El Arish, respectively. While the percentage of occurrences during the coldest hours (mean-2*standard deviation) was 3.46% (<9.86°C), 3.26% (<12.07°C), 3.42% (<11.96°C), 4.03% (<11.35°C) and 4.31% (<9.76°C) over Marsa Matrouh, Ras El-Tin, Abu Qir, Port Said and El Arish, respectively. as shown in Fig. (6).

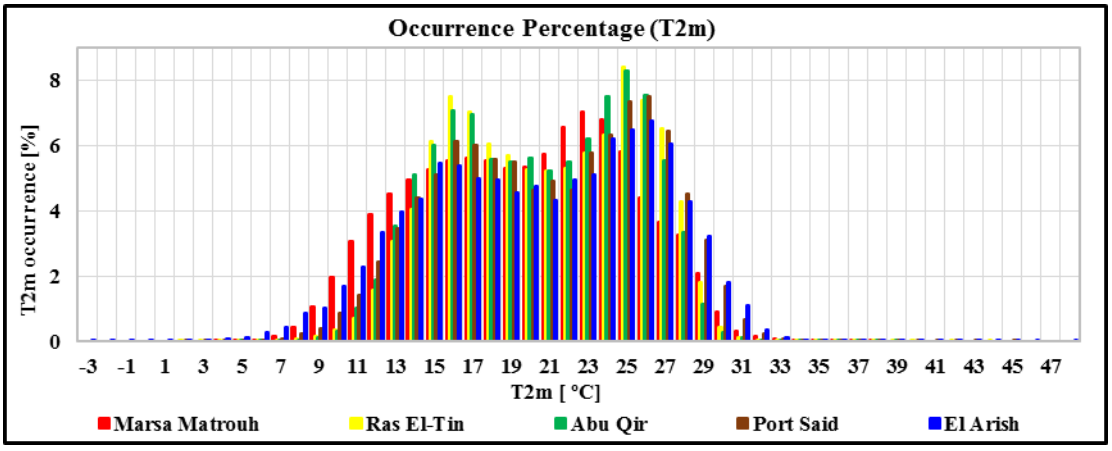

Fig. 6. The occurrence percentage of the parameters understudy based on hourly Corrected ERA5 data (1979-2023) along the study area

3. Heatwaves analysis

3.1 Number of annual hot days

Table (6) and Fig. (7) reveal a significant positive trend in annual hot days across all five studied stations (Marsa Matrouh, Ras El-Tin, Abu Qir, Port Said, and El Arish) during 1979-2023. The data show an overall increase in hot days at all stations, categorized by mild, moderate, severe, and extreme thresholds. Marsa Matrouh has the smallest increase (1.09 days/year), while Port Said shows the largest (1.80 days/year) in the mild category. While the number of hot days' rises across all thresholds, the increase slows for more extreme categories. For example, the number of severe and extremely hot days grows more slowly than mild or moderate hot days. This suggests that although extreme heat events remain less frequent, moderate to severe hot days are becoming more

common, reflecting the broader trend of rising temperatures and heat extremes due to climate change.

Table 6. Annual hot days number trend during the period (1979-2023) over Marsa Matrouh, Ras El-Tin, Abu Qir, Port Said and El Arish under mild, moderate, severe, and extreme basis

Station	Trend (day / year)			
	Mild (> 85% Percentile)	Moderate (> 90% Percentile)	Severe (> 95% Percentile)	Extreme (> 99% Percentile)
Marsa Matrouh	1.09	0.69	0.23	0.01
Ras El-Tin	1.69	1.39	0.77	0.04
Abu Qir	1.66	1.20	0.53	0.03
Port Said	1.80	1.50	0.74	0.08
El Arish	1.71	1.31	0.57	0.03

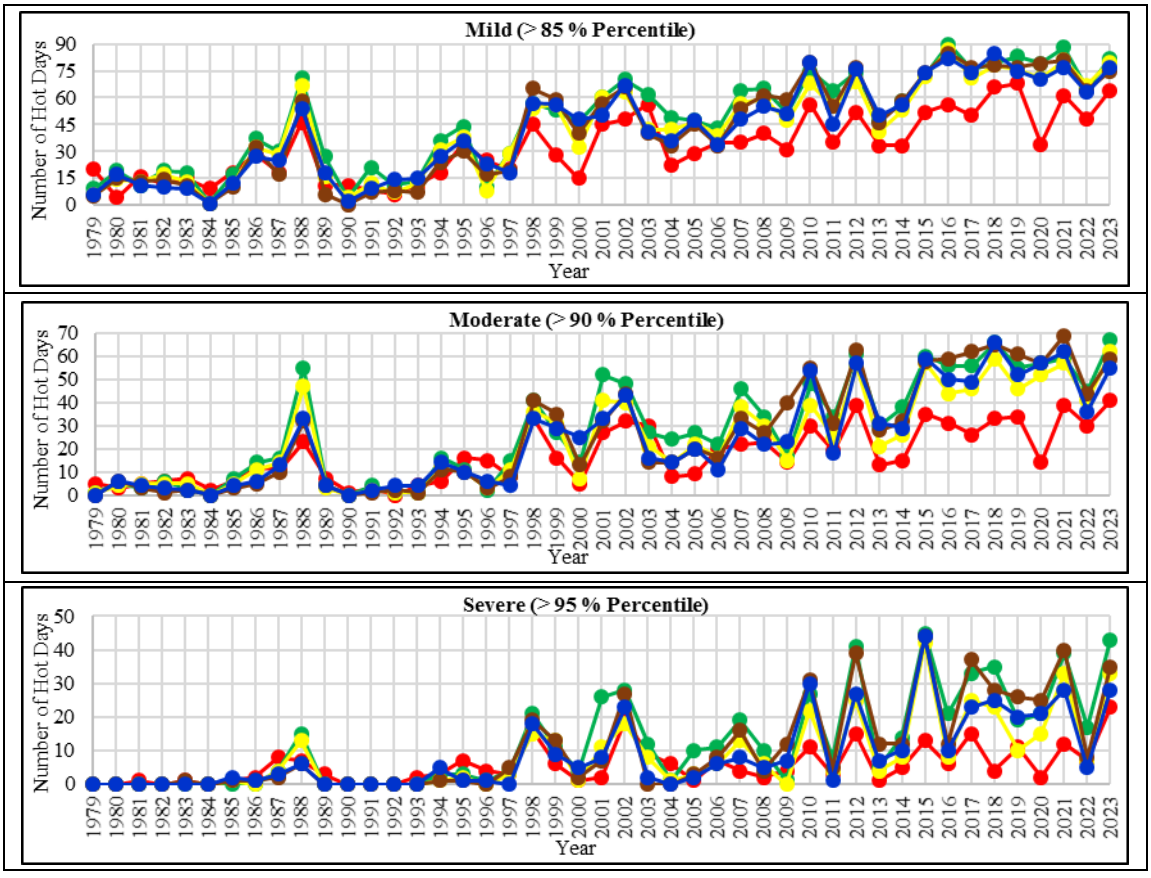

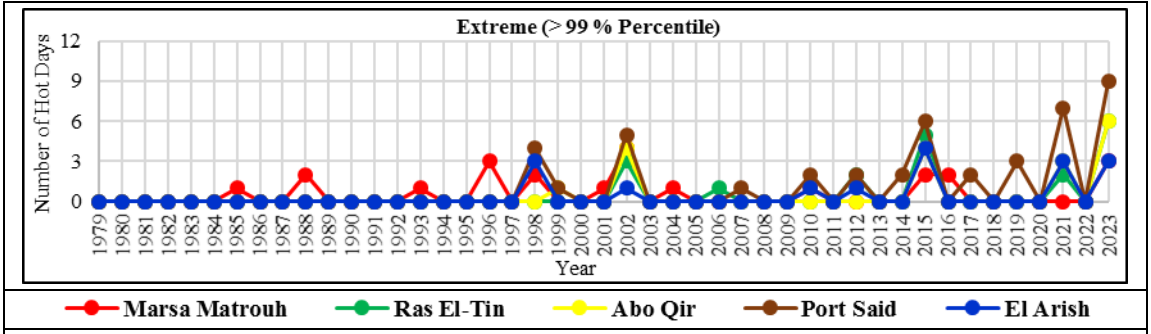

Fig. 7. Number of annual hot days during the period, 1979-2023

3.2 Heatwave frequency

Table (7) and Fig. (8) display the trend in heatwave frequency (events per year) from 1979 to 2023 for all studied stations, categorized by intensity levels: mild (above the 85th percentile), moderate (above the 90th percentile), severe (above the 95th percentile), and extreme (above the 99th percentile).

All stations show an upward trend in heatwave frequency across all thresholds, indicating an increase in heatwave events. Mild heatwaves exhibit a modest rise (0.09 to 0.11 events/year), while moderate and severe heatwaves show a more notable increase (0.12 to 0.17 events/year). Port Said and El Arish record the highest increases, especially in the moderate and severe categories. Ras El-Tin, though showing a smaller rise in mild heatwaves (0.02 events/year), experiences a significant increase in the moderate and severe categories.

Extreme heatwaves remain rare, with most stations showing a slower rise (0.01 events/year), but their gradual increase suggests a growing risk. Overall, the study highlights a clear intensification of heatwaves, particularly in the moderate and severe categories, in line with global warming trends.

Table 7. Heatwave frequency trend during the period (1979-2023) over Marsa Matrouh, Ras El-Tin, Abu Qir, Port Said and El Arish under mild, moderate, severe, and extreme basis

Station	Trend (event / year)			
	Mild (> 85% Percentile)	Moderate (> 90% Percentile)	Severe (> 95% Percentile)	Extreme (> 99% Percentile)
Marsa Matrouh	0.11	0.12	0.05	0.01
Ras El-Tin	0.02	0.14	0.12	0.01
Abu Qir	0.07	0.14	0.11	0.01
Port Said	0.11	0.17	0.15	0.01
El Arish	0.09	0.16	0.12	0.01

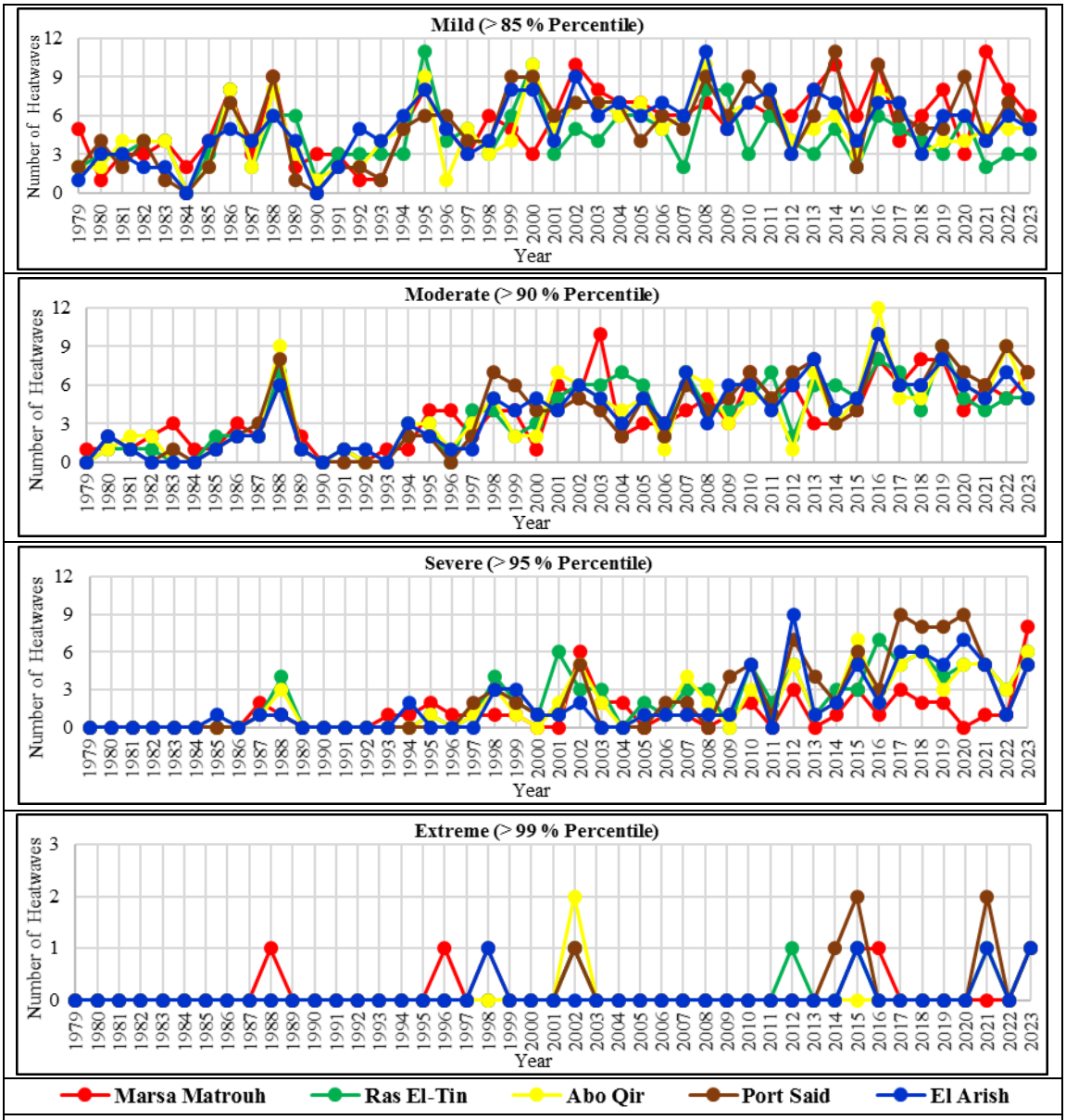

Fig. 8. (Heatwave Frequency) Number of Heatwaves events occurring in a specific time frame (Year) during the period, 1979-2023

3.3 Heatwave duration

Table (8) and Fig. (9) present trends in heatwave duration (days per year) from 1979 to 2023, categorized by intensity levels (mild, moderate, severe, extreme) across five locations: Marsa Matrouh, Ras El-Tin, Abu Qir, Port Said, and El Arish. The results show an increasing duration of heatwaves at all stations, with regional differences.

Mild heatwaves (>85th percentile) show a steady rise, with Port Said experiencing the highest increase (1.82 days/year) and Marsa Matrouh the lowest (1.07 days/year). This suggests that mild heatwaves are becoming longer over time.

Moderate heatwaves (>90th percentile) also demonstrate an upward trend, with Ras El-Tin and Port Said recording the highest increases (1.34 and 1.42 days/year,

respectively). This indicates that moderate heatwaves are not only more frequent but also more persistent.

Severe heatwaves (>95th percentile) exhibit a gradual rise in duration across all stations, with the highest increases in Ras El-Tin (0.69 days/year) and Port Said (0.65 days/year), suggesting that severe heatwaves are becoming longer-lasting.

Extreme heatwaves (>99th percentile) remain rare but show a slight increase in duration, particularly in Port Said (0.04 days/year).

Overall, the study highlights a clear trend of increasing heatwave duration, especially for moderate and severe categories, with potential implications for public health, infrastructure, and climate adaptation.

Table 8. Heatwave duration trend during the period (1979-2023) over Marsa Matrouh, Ras El-Tin, Abu Qir, Port Said and El Arish under mild, moderate, severe, and extreme basis

Station	Trend (day / year)			
	Mild (> 85% Percentile)	Moderate (> 90% Percentile)	Severe (> 95% Percentile)	Extreme (> 99% Percentile)
Marsa Matrouh	1.07	0.62	0.16	0.01
Ras El-Tin	1.71	1.34	0.69	0.02
Abu Qir	1.65	1.15	0.47	0.01
Port Said	1.82	1.42	0.65	0.04
El Arish	1.71	1.25	0.47	0.02

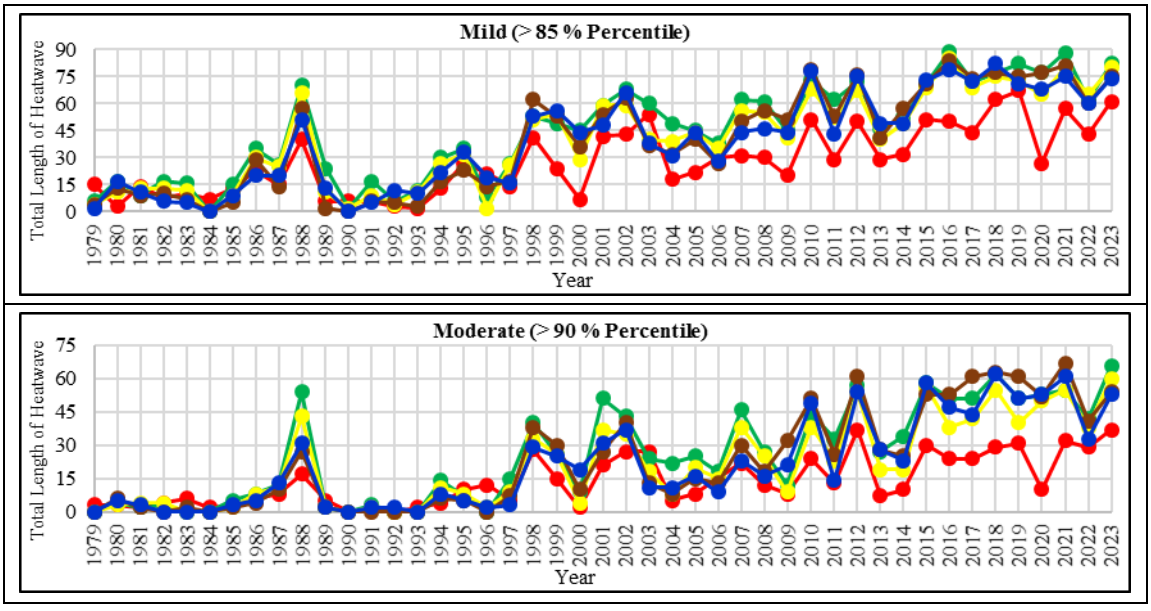

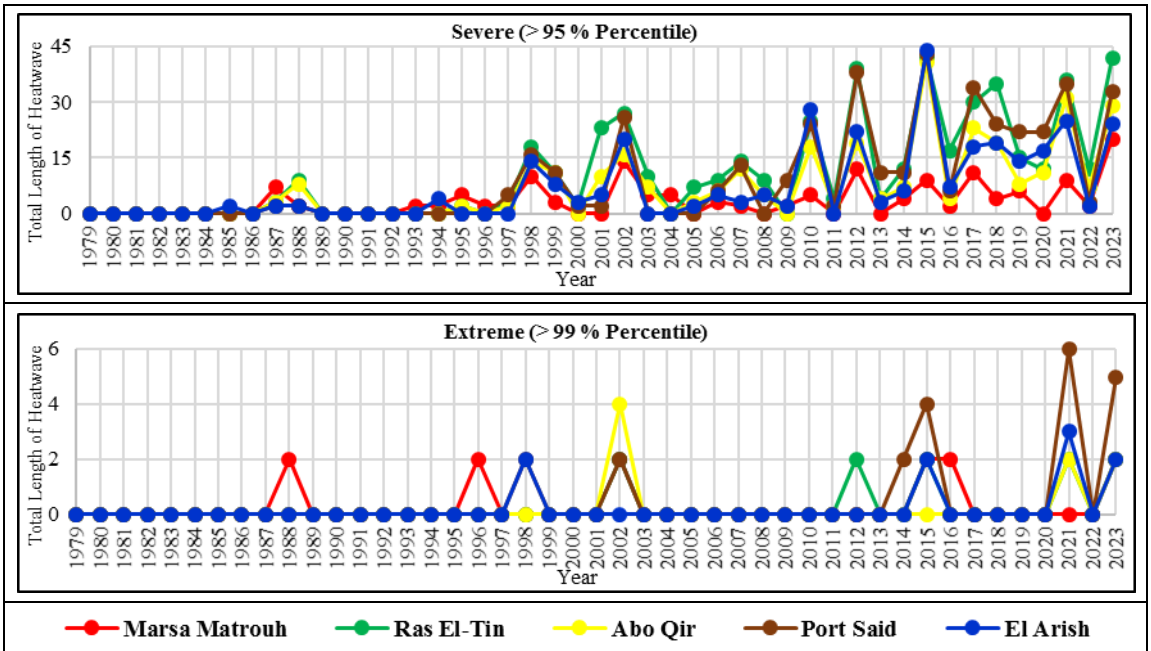

Fig. 9. (Heatwave Duration) Total number of consecutive days that constitute a heatwave during the period, 1979-2023

3.4 Heatwave intensity

Table (9) and Fig. (10) present trends in heatwave intensity (˚C/day) across five stations (Marsa Matrouh, Ras El-Tin, Abu Qir, Port Said, and El Arish) during 1979-2023, for mild, moderate, severe, and extreme heatwave categories.

Mild Heatwaves (>85% Percentile): Intensity increases slightly across all stations, with Port Said and El Arish showing the highest rates (0.06˚C/day). Marsa Matrouh exhibits the lowest rate (0.01˚C/day), indicating a slower warming trend for mild heatwaves in this area.

Moderate Heatwaves (>90% Percentile): Similar to mild heatwaves, intensity increases modestly. Port Said and Ras El-Tin record higher trends (0.055˚C/day and 0.049˚C/day, respectively), suggesting a slight rise in the rate of temperature change as heatwaves intensify from mild to moderate. Marsa Matrouh shows the lowest increase in intensity (0.008˚C/day).

Severe Heatwaves (>95% Percentile): Intensity increases notably, with Port Said and El Arish showing the highest rates (0.050˚C/day). Marsa Matrouh, although less pronounced, also shows a moderate increase (0.046˚C/day). This reflects faster warming during severe heatwaves.

Extreme Heatwaves (>99% Percentile): Extreme heatwaves exhibit the highest intensity increase. Port Said and El Arish have the sharpest rise (0.020˚C/day and 0.021˚C/day, respectively), though all stations show an increase over time. Marsa Matrouh shows a slower increase (0.015˚C/day).

In conclusion, heatwave intensity is rising across all stations, with Port Said and El Arish experiencing the highest rates of increase. Mild heatwaves have shown moderate

intensity growth, while severe and extreme events have intensified more significantly. These trends align with global warming, highlighting the growing risk and impact of heatwaves in the region, necessitating adaptation strategies for public health, infrastructure, and ecosystems.

Table 9. Heatwave intensity trend during the period (1979-2023) over Marsa Matrouh, Ras El-Tin, Abu Qir, Port Said and El Arish under mild, moderate, severe, and extreme basis

Station	Trend (˚C / day of event)			
	Mild (> 85% Percentile)	Moderate (> 90% Percentile)	Severe (> 95% Percentile)	Extreme (> 99% Percentile)
Marsa Matrouh	0.01	0.008	0.046	0.015
Ras El-Tin	0.05	0.049	0.044	0.032
Abu Qir	0.04	0.039	0.042	0.013
Port Said	0.06	0.055	0.050	0.020
El Arish	0.06	0.053	0.050	0.021

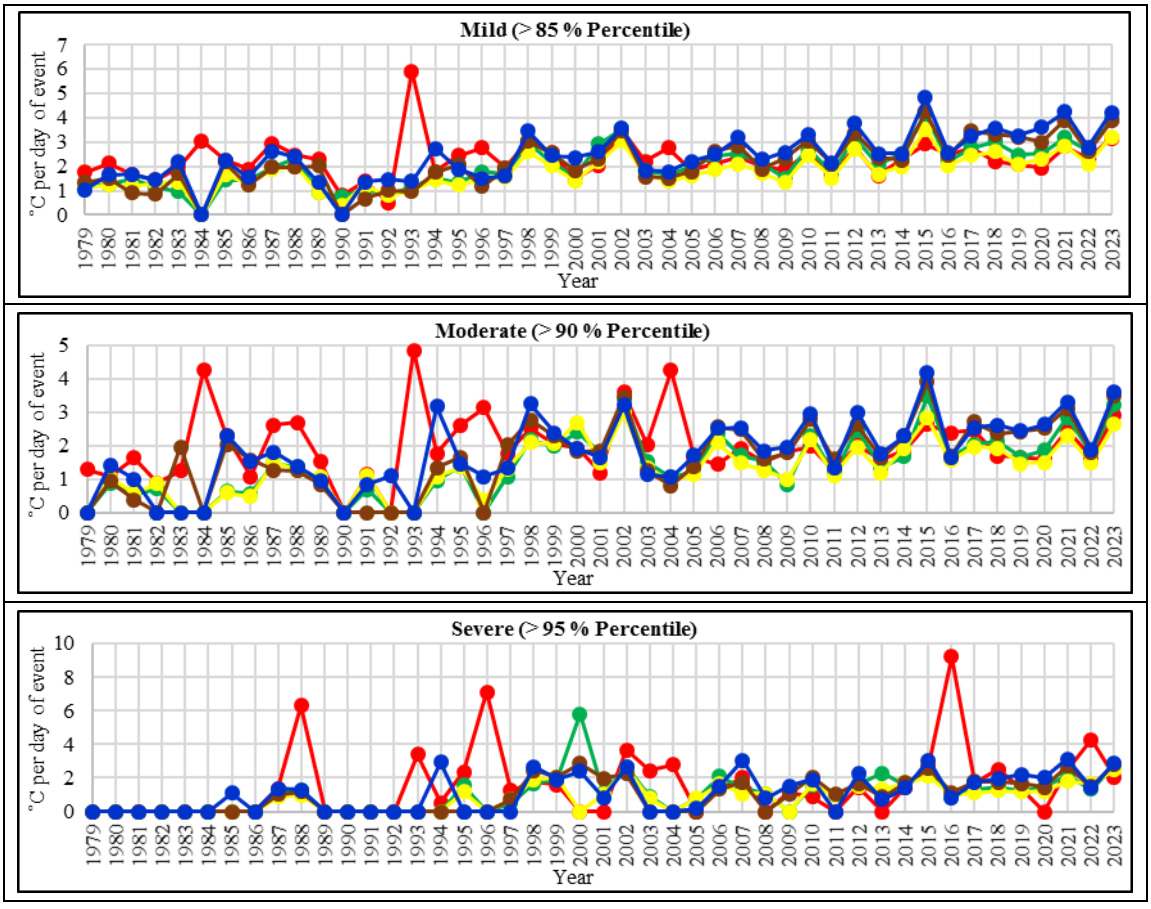

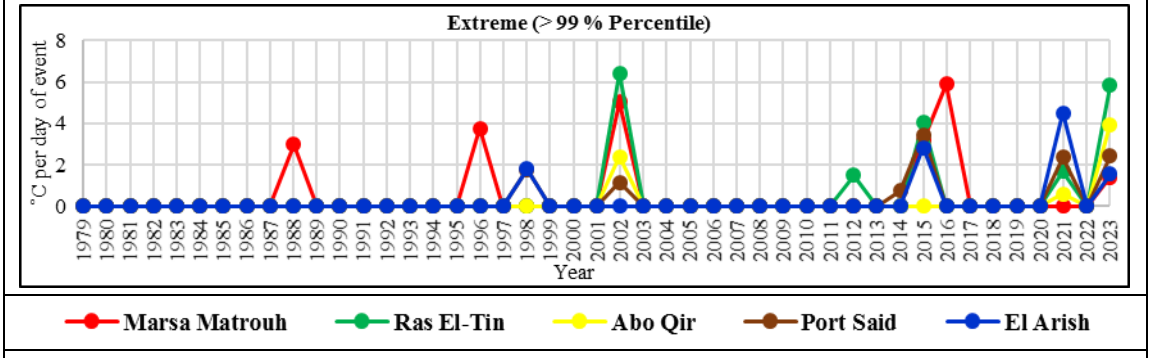

Fig. 10. (Heatwave Intensity) Average Severity of heatwaves (Above maximum/minimum) during the period, 1979-2023

3.5 Heatwave appearance period

Table (10) and Fig. (11) present trends in heatwave appearance periods (measured in days per year) across four intensity categories (Mild, Moderate, Severe, and Extreme) during 1979-2023 at five stations: Marsa Matrouh, Ras El-Tin, Abu Qir, Port Said, and El Arish. The data reveal a clear upward trend in the duration of heatwaves across all stations, with some regions experiencing more pronounced increases.

Mild Heatwaves: Mild heatwaves have shown significant increases in duration, with Port Said exhibiting the highest rise (2.17 days/year), followed by Abu Qir (1.60 days/year) and El Arish (1.78 days/year). Marsa Matrouh shows a slower increase (1.18 days/year), reflecting a regional difference in the rate of change. Notably, Port Said and Marsa Matrouh reported the longest mild heatwave duration (121 days) in 2010, highlighting extended periods of heat stress in the region.

Moderate Heatwaves: Moderate heatwaves show similar upward trends, with Ras El-Tin (1.66 days/year) and Port Said (1.88 days/year) experiencing the largest increases. The data from 2016 show significant rises in duration, such as 88 days in Port Said and 120 days in Marsa Matrouh. These increases point to a growing intensity and persistence of moderate heat events, particularly in coastal regions.

Severe Heatwaves: Severe heatwaves have increased moderately, with Port Said and Ras El-Tin showing the highest trends (1.26 and 1.27 days/year, respectively). Although the increase is smaller compared to milder categories, it signals a growing frequency of extreme temperature events. For example, in 2015, El Arish experienced severe heatwaves lasting up to 56 days, suggesting more prolonged extreme heat periods.

Extreme Heatwaves: Extreme heatwaves show the smallest rate of increase in duration (0.01-0.05 days/year), but significant rises are noted in recent years, especially in 2016 (Port Said, 30 days) and 2022 (Marsa Matrouh, 57 days). Despite their rarity, extreme heatwaves have become more persistent, posing increasing risks to health and agriculture.

Overall, heatwaves in the study region have become more frequent and persistent, with the most significant increases observed in the moderate, severe, and extreme categories. This trend suggests a growing intensity of heat events, particularly over the

last two decades. These findings underscore the need for climate adaptation strategies, particularly in vulnerable coastal regions prone to prolonged and intense heat.

Table 10. Heatwave appearance period trend during the period (1979-2023) over Marsa Matrouh, Ras El-Tin, Abu Qir, Port Said and El Arish under mild, moderate, severe, and extreme basis.

Station	Trend (day / year)			
	Mild (> 85% Percentile)	Moderate (> 90% Percentile)	Severe (> 95% Percentile)	Extreme (> 99% Percentile)
Marsa Matrouh	1.18	1.30	0.46	0.01
Ras El-Tin	1.43	1.66	1.27	0.01
Abu Qir	1.60	1.57	1.17	0.01
Port Said	2.17	1.88	1.26	0.05
El Arish	1.78	1.72	1.00	0.01

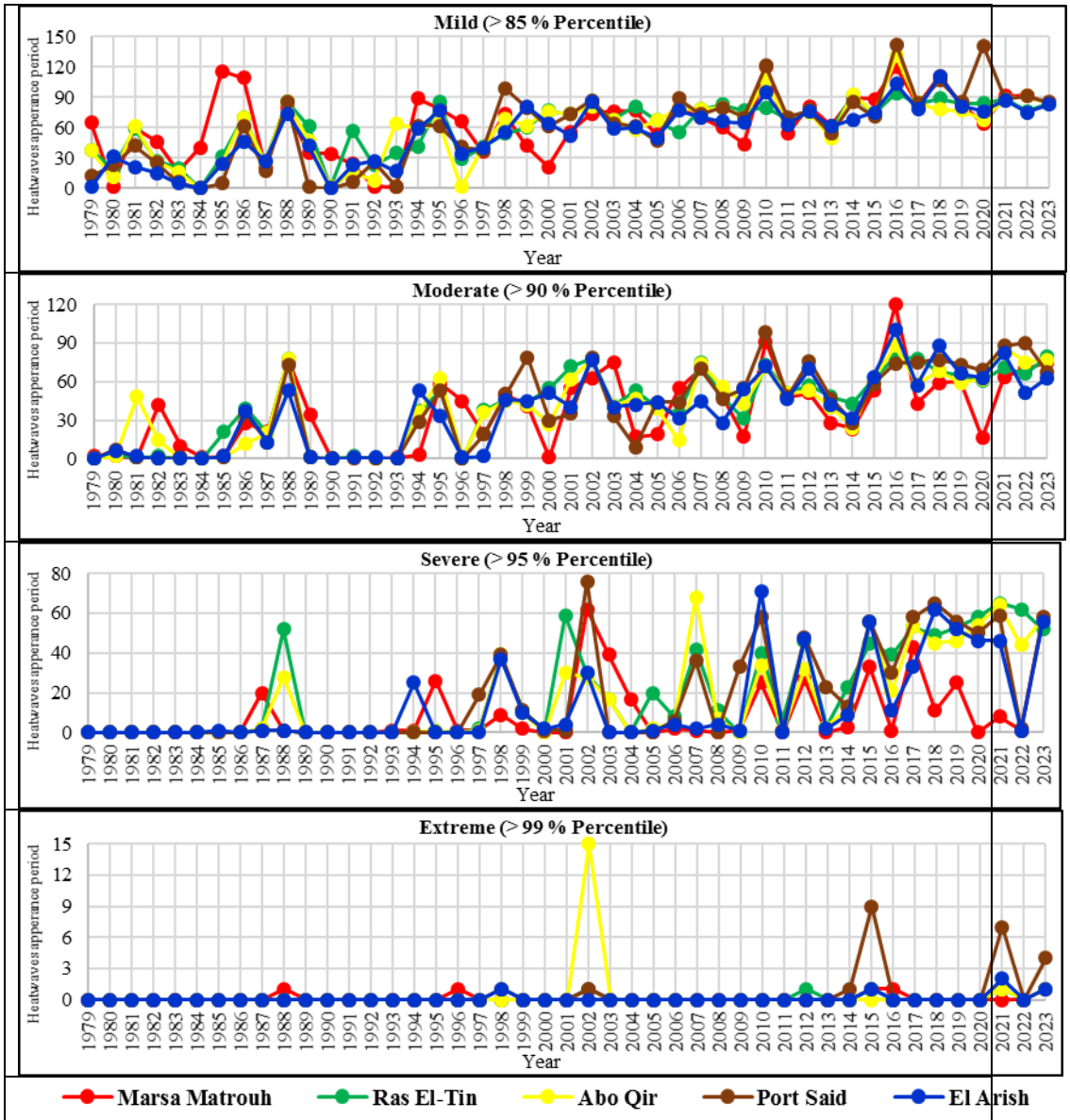

Fig. 11. (Heatwave appearance period) The period of the onset and the ending heatwaves over the years during the period, 1979-2023

3.6 The onset and the ending of the heatwaves over the years

Fig. (12) presents the first and last days of heatwaves from 1979 to 2023 at five stations (Marsa Matrouh, Ras El-Tin, Abu Qir, Port Said, and El Arish) across various heatwave intensity categories. The data highlight the increasing duration and frequency of heatwaves, with heatwaves starting earlier and lasting longer as the years progress, consistent with rising global temperatures.

Heatwave duration and trends: Marsa Matrouh, Ras El-Tin, and Port Said show significant increases in heatwave duration over time. For example, in 2023, Marsa Matrouh experienced heatwaves from day 188 to day 272, indicating a longer period of heat stress compared to earlier years. Similarly, Port Said and El Arish exhibit extended heatwave periods in recent decades. In contrast, Abu Qir and Ras El-Tin show variability, with certain years like 1996 and 2001 having exceptionally long durations.

Yearly variation and anomalies: Certain years, such as 1993 and 2015, stand out for having particularly prolonged heatwaves. In 2018, El Arish and Port Said experienced heatwaves from day 186 to day 297 and day 186 to day 273, respectively, indicating extended and intense heat events. Some years, like 1990, 2000, and 2011, show missing or incomplete data, possibly due to local anomalies or reporting issues.

Comparative analysis among stations: Marsa Matrouh generally exhibits consistent heatwave trends, with start dates between days 168 and 234 and end dates between 233 and 295, though some variability is seen in 2020–2023. Port Said experiences some of the earliest start dates and longest heatwave durations, particularly in 2010 and 2015, suggesting a rising heat exposure in coastal regions. Ras El-Tin and Abu Qir also show increasing heatwave durations, especially since 2010, with notable heatwave expansions in 2015.

Long-term climate change signals: The trends reflect the broader impact of climate change, with increasing heatwave frequency and duration, linked to warming trends, changes in atmospheric circulation, and shifts in sea surface temperatures. The most recent years (2020-2023) show heatwaves starting earlier and lasting longer, particularly in Port Said, Marsa Matrouh, and El Arish.

The data show a clear trend toward longer and more intense heatwave periods, likely driven by climate change. These findings underline the importance of adaptation strategies to mitigate the impacts of extended heat events on health, infrastructure, and ecosystems in vulnerable regions like coastal Egypt.

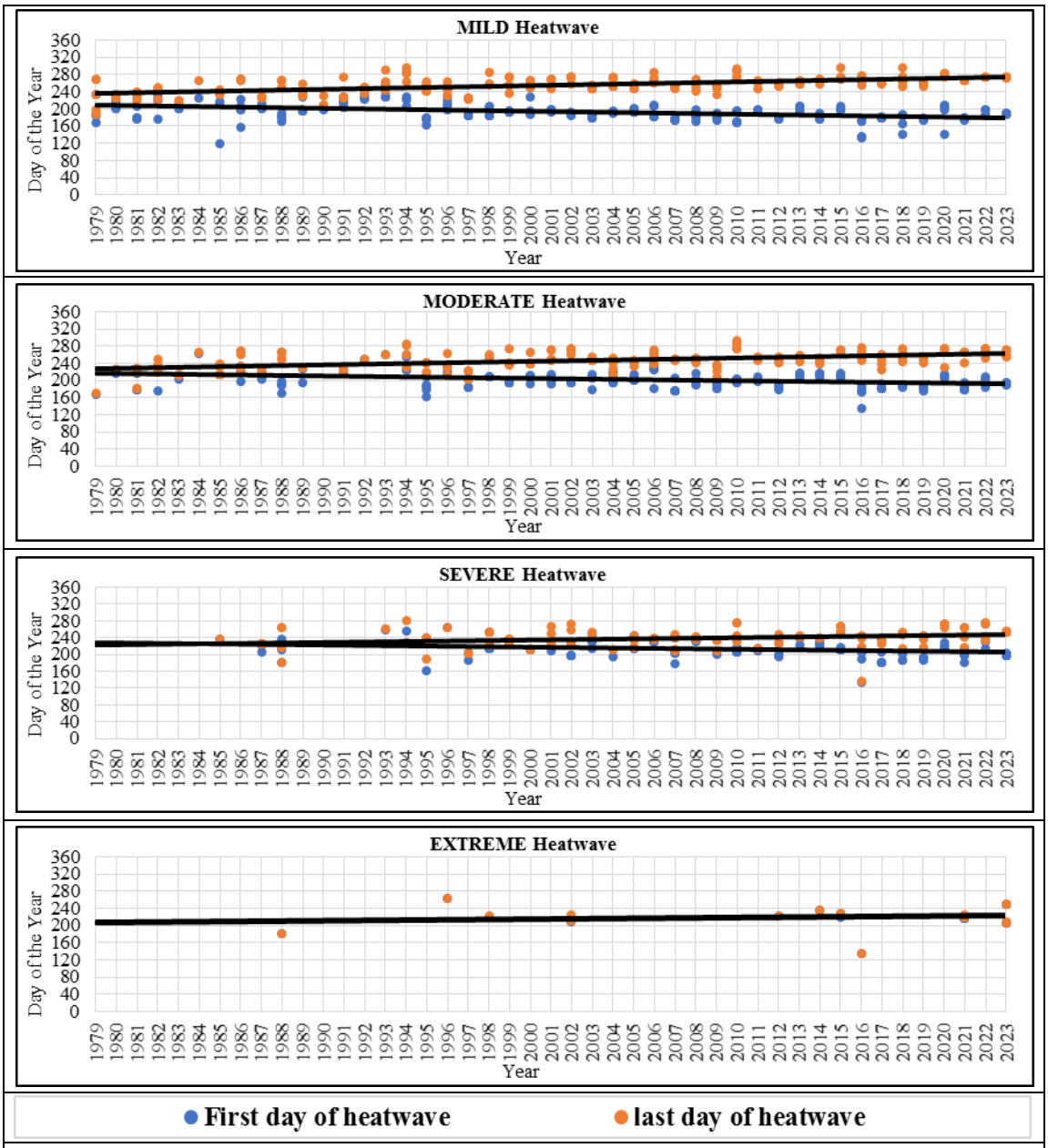

Fig. 12. The onset and the ending of the heatwaves over the years during the period, 1979-2023

CONCLUSION

This study provides a comprehensive analysis of surface air temperature trends and heatwave characteristics along the Egyptian Mediterranean Coast (EMC) over a period spanning from 1979 to 2023. The findings clearly indicate that climate change is significantly altering the temperature patterns in this region, with increased frequency, intensity, and duration of heatwaves becoming more evident over time. These changes are particularly pronounced in the coastal cities of Port Said and El Arish, which have shown the most rapid warming and highest increases in heatwave events.

The use of observational data and ERA5 reanalysis data allowed for an in-depth examination of temperature fluctuations, validation of the reanalysis dataset, and bias correction to enhance the accuracy of long-term climate projections. The successful application of cumulative distribution function (CDF) bias correction to ERA5 data improved the precision of the long-term temperature trends, confirming that ERA5 is a reliable source for describing long-term surface air temperature variations in the region.

One of the key findings of this study is the significant positive monotonic trend in annual average temperatures, with a spatial variation across the five locations studied. Over the 45-year period (1979-2023), all five locations experienced warming, with the greatest warming observed at El Arish, at a rate of 0.06°C per decade. This warming trend aligns with the increasing occurrence of hot days and heatwaves, particularly in the last two decades. As the region continues to warm, the number of mild, moderate, and severe heatwave days is projected to increase, with the most significant changes in moderate and severe categories.

Heatwaves have become longer and more intense across the study region, and this trend is expected to continue under future climate change scenarios. The duration of heatwaves has notably increased in the past two decades, with regions like Port Said and El Arish seeing the most substantial rises in the number of heatwave days. These areas have also experienced longer periods of extreme heat, particularly since 2010. For example, in 2015, Port Said experienced a severe heatwave lasting over 50 days, underscoring the growing intensity of heat events. The frequency of extreme heatwaves, although still rare, has shown a steady increase over time, posing significant risks to public health, agriculture, and infrastructure.

Moreover, the study highlights the diurnal and seasonal variations in temperature patterns. The highest temperatures are typically observed in August, with a pronounced daily cycle, where the maximum temperatures occur between 1200 and 1300, and the minimum temperatures are recorded between 0400 and 0500. The annual temperature cycle shows that temperatures reach their peak in the summer months and dip to their lowest in the winter, but the amplitude of this cycle is increasing as global temperatures rise. These patterns suggest that the risk of heat exposure is likely to become more severe, particularly during the warmer months.

The increasing frequency and intensity of heatwaves in the EMC have serious implications for climate resilience. Heatwaves not only impact human health by exacerbating conditions like heat stress and heatstroke but also pose significant risks to ecosystems, agriculture, and infrastructure. Prolonged heat events can strain energy and water resources, increase the demand for cooling systems, and reduce agricultural productivity due to heat stress on crops. Coastal areas, which are particularly vulnerable to heatwaves due to their lower elevation and high population density, may also experience enhanced urban heat island effects, further exacerbating the risks of extreme heat.

In response to these growing challenges, it is critical that policymakers, urban planners, and public health officials develop robust adaptation strategies to mitigate the

impacts of heatwaves. These strategies should focus on enhancing climate resilience through improved infrastructure, such as the development of cooling centers, shaded areas, and green spaces to reduce the urban heat island effect. Additionally, early warning systems and heat action plans should be established to safeguard vulnerable populations during extreme heat events.

There is also a need for increased public awareness regarding the risks associated with heatwaves and the importance of climate adaptation. Educating the public about how to reduce exposure to extreme heat and encouraging the use of adaptive measures, such as wearing appropriate clothing, staying hydrated, and minimizing outdoor activities during peak heat hours, will be critical to reducing the health impacts of rising temperatures.

Furthermore, sustainable urban development and effective land-use planning can help mitigate the effects of heatwaves in coastal regions. Integrating climate change considerations into urban planning, including the promotion of energy-efficient building designs, the use of reflective and heat-resistant materials, and the establishment of green infrastructure, can help cities adapt to the changing climate and reduce the heat-related risks.

The results of this study also call for greater investment in climate research and monitoring to better understand the long-term impacts of climate change on heatwaves in coastal Egypt. Continuous monitoring and the development of high-resolution climate models are essential for improving climate predictions and informing future adaptation strategies. Monitoring the interactions between sea surface temperatures, atmospheric circulation patterns, and heatwaves will provide valuable insights into the mechanisms driving the increasing intensity of heat events in the EMC.

In conclusion, the study demonstrates that the Egyptian Mediterranean Coast is experiencing a clear and significant warming trend, with an increased frequency, intensity, and duration of heatwaves. These changes will have far-reaching consequences for public health, ecosystems, and infrastructure in the region. To address these challenges, it is essential to implement adaptive strategies that enhance resilience and minimize the impacts of heatwaves. As global temperatures continue to rise, the need for proactive climate adaptation in vulnerable regions like Egypt's Mediterranean coast becomes more pressing.

REFERENCES

- **Aboelkhair, H.; Mohamed, B.; Morsy, M. and Nagy, H. (2023).** Co-Occurrence of Atmospheric and Oceanic Heatwaves in the Eastern Mediterranean over the Last Four Decades. *Remote Sensing, 15*(7), 1841. https://doi.org/10.3390/rs15071841
- **Alcamo, J.; Moreno, J. M.; Novaky, B.; Bindi, M.; Corobov, R.; Devoy, R. J. N; giannakopoulos, C.; Martin, E.; Olesen, J. E. and Shvidenko, A. (2007).** Europe. Climate Change 2007: Impacts, adaptation, and vulnerability. Contribution by Working Group II to the Fourth Assessment Report of the Intergovernmental Panel on Climate Change, edited by **Parry, M. L.; Canziani, O. F.; Palutikof, J. P.; van**

der Linden, P. J. and Hanson, C. E., Cambridge University Press, Cambridge, UK,541-580.

- **Alpert, P.; Krichak, S. O.; Shafir, H.; Haim, D. and Osetinsky, I. (2008).** Climatic trends in extremes employing regional modeling and statistical interpretation over the E. Mediterranean. *Global and Planetary Change, 63*(2-3), 163-170. https://doi.org/10.1016/j.gloplacha.2008.03.003
- **Anagnostou E. N.; Negri A. J. and Adler R. F. (1999)**. Statistical adjustment of satellite microwave monthly rainfall estimates over Amazonia, *Journal of Applied Meteorology*, *38,* 1590-1598.
- **Bawadekji, A.; Tonbol, K.; Ghazouani, N.; Becheikh, N. and Shaltout, M. (2022)**. Recent atmospheric changes and future projections along the Saudi Arabian Red Sea Coast. *Scientific Reports*, *12*(1). https://doi.org/10.1038/s41598-021-04200-z
- **Bucchignani, E.; Mercogliano, P.; Panitz, H. J. and Montesarchio, M. (2018).** Climate change projections for the Middle East-North Africa domain with COSMO-CLM at different spatial resolutions. *Advances in Climate Change Research*, *9*(1), 66-80. https://doi.org/10.1016/j.accre.2018.01.004
- **Clark, J. P. and Feldstein, S. B. (2020).** What drives the North Atlantic oscillation's temperature anomaly pattern? Part I: The growth and decay of the surface air temperature anomalies. *Journal of the Atmospheric Sciences, 77*(1), 185-198. https://doi.org/10.1175/JAS-D-19-0027.1
- **De Vries, A. J.; Tyrlis, E.; Edry, D.; Krichak, S. O.; Steil, B. and Lelieveld, J. (2013).** Extreme precipitation events in the Middle East: Dynamics of the Active Red Sea Trough. *Journal of Geophysical Research Atmospheres, 118*(13), 7087-7108. https://doi.org/10.1002/jgrd.50569
- **Domroes, M. and El-Tantawi, A. (2005).** Recent temporal and spatial temperature changes in Egypt. *International Journal of Climatology, 25*(1), 51-63. https://doi.org/10.1002/joc.1114
- **Elbessa, M.; Abdelrahman, S. M.; Tonbol, K. and Shaltout, M. (2021)**. Dynamical downscaling of surface air temperature and wind field variabilities over the southeastern levantine basin, mediterranean sea. *Climate*, *9*(10). https://doi.org/10.3390/cli9100150
- **Elbessa, M. and Shaltout, M. (2024)**. Statistical downscaling of global climate projection along the Egyptian Mediterranean coast. Oceanologia, 66(4). 66401. https://doi.org/10.5697/OBOE5006
- **Eldeeb, A. R. and Elemam, D. A. (2022).** Climate Change in the Coastal Areas: Consequences, Adaptations, and Projections for the Northern Coastal Area, Egypt. *Scientific Journal for Damietta Faculty of Science, 13*(2), 19-29. https://sjdfs.journals.ekb.eg/
- **El-Geziry, T. M.; Elbessa, M. and Tonbol, K. M. (2021).** Climatology of Sea-Land Breezes Along the Southern Coast of the Levantine Basin. *Pure and Applied Geophysics, 178*(5), 1927-1941. https://doi.org/10.1007/s00024-021-02726-x
- **Gado, T. A. and El-Agha, D. E. (2021).** Climate Change Impacts on Water Balance in Egypt and Opportunities for Adaptations. *In Springer Water* (pp. 13-47). Springer Nature. https://doi.org/10.1007/978-3-030-78574-1_2

- **Gentilucci, M.; Moustafa, A. A.; Abdel-Gawad, F. K.; Mansour, S. R.; Coppola, M. R.; Caserta, L.; Inglese, S.; Pambianchi, G. and Guerriero, G. (2021).** Advances in egyptian mediterranean coast climate change monitoring. *Water (Switzerland), 13*(13). https://doi.org/10.3390/w13131870
- **Haggag, M. and El-Badry, H. (2013).** Mesoscale Numerical Study of Quasi-Stationary Convective System over Jeddah in November 2009. *Atmospheric and Climate Sciences, 03*(01), 73-86. https://doi.org/10.4236/acs.2013.31010
- **Hersbach, H.; Bell, B.; Berrisford, P.; Hirahara, S.; Horányi, A.; Muñoz-Sabater, J.; Nicolas, J.; Peubey, C.; Radu, R.; Schepers, D.; Simmons, A.; Soci, C.; Abdalla, S.; Abellan, X.; Balsamo, G.; Bechtold, P.; Biavati, G.; Bidlot, J.; Bonavita, M.; … Thépaut, J. N. (2020)**. The ERA5 global reanalysis. *Quarterly Journal of the Royal Meteorological Society, 146*(730), 1999-2049. https://doi.org/10.1002/qj.3803
- **Ibrahim, O.; Mohamed, B. and Nagy, H. (2021).** Spatial Variability and Trends of Marine Heat Waves in the Eastern Mediterranean Sea over 39 Years. *Journal of Marine Science and Engineering, 9*(6), 643. https://doi.org/10.3390/jmse9060643
- **IPCC. (2014).** Climate change 2014: impacts, adaptation, and vulnerability: Working Group II contribution to the fifth assessment report of the Intergovernmental Panel on Climate Change, edited by **Field, C. B. and Barros, V. R.**, Cambridge University Press.
- **IPCC. (2019).** Special Report - Global Warming of 1.5°C, Report of the Intergovernmental Panel on Global Warming https://www.ipcc.ch/sr15/
- **Kautz, L. A.; Martius, O.; Pfahl, S.; Pinto, J. G.; Ramos, A. M.; Sousa, P. M. and Woollings, T. (2022).** Atmospheric blocking and weather extremes over the Euro-Atlantic sector - A review in *Weather and Climate Dynamics* (Vol. 3, Issue 1, pp. 305-336). Copernicus Publications. https://doi.org/10.5194/wcd-3-305-2022
- **Kendall M.G. (1975)**. Rank Correlation Methods, 4th edition. Charles Griffin, London, UK.
- **Lelieveld, J.; Proestos, Y.; Hadjinicolaou, P.; Tanarhte, M.; Tyrlis, E. and Zittis, G. (2016).** Strongly increasing heat extremes in the Middle East and North Africa (MENA) in the 21st century. *Climatic Change, 137*(1-2), 245-260. https://doi.org/10.1007/s10584-016-1665-6
- **Lionello, P.; Bhend, J.; Buzzi, A.; Della-Marta, P. M.; Krichak, S. O.; Jansà, A.; Maheras, P.; Sanna, A.; Trigo, I. F. and Trigo, R. (2006).** Chapter 6 Cyclones in the Mediterranean region: Climatology and effects on the environment. *Developments in Earth and Environmental Sciences, 4*(C), 325-372. https://doi.org/10.1016/S1571-9197(06)80009-1
- **Mahfouz, B. M. B.; Osman, A. G. M.; Saber, S. A. and Kanhalaf-Allah, H. M. M. (2020).** Assessment of weather and climate variability over the western harbor of Alexandria, Egypt. *Egyptian Journal of Aquatic Biology and Fisheries, 24*(5), 323-339. https://doi.org/10.21608/EJABF.2020.105861
- **Mann H.B. (1945)**. Non-parametric test against trend, Econometrica 13, 245-259. doi: 10.2307/1907187
- **Mostafa, S. M.; Wahed, O.; El-Nashar, W. Y.; El-Marsafawy, S. M. and Abd-Elhamid, H. F. (2021).** Impact of climate change on water resources and crop yield in the

middle Egypt region. *Aqua Water Infrastructure, Ecosystems and Society, 70*(7), 1066–1084. https://doi.org/10.2166/aqua.2021.019

- **Nastos, P. T. and Zerefos, C. S. (2009).** Spatial and temporal variability of consecutive dry and wet days in Greece. *Atmospheric Research, 94*(4), 616-628. https://doi.org/10.1016/j.atmosres.2009.03.009
- **Pastor, F. and Khodayar, S. (2023).** Marine heat waves: Characterizing a major climate impact in the Mediterranean. *Science of the Total Environment,* 861. https://doi.org/10.1016/j.scitotenv.2022.160621
- **Reichle R. H. and Koster, R. D. (2004)**. Bias reduction in short records of satellite soil moisture. *Geophysical Research Letters, 31*(19). https://doi.org/10.1029/2004GL020938.
- **Saaroni, H.; Bitan, A.; Alpert, P. and Ziv, B. (1996).** Continental polar outbreaks into the Levant and eastern Mediterranean. *international journal of climatology, 16*, 1175-1191. https://doi.org/10.1002/(SICI)1097-0088(199610)16:10<1175:AID-JOC79>3.0.CO;2
- **Saaroni, H.; Ziv, B.; Bitan, A. and Alpert, P. (1998).** Easterly wind storms over Israel. *Theoretical and Applied Climatology, 59*(1-2), 61-77. https://doi.org/10.1007/s007040050013
- **Shaltout, M.; El Gindy, A. and Omstedt, A. (2013).** Recent climate trends and future scenarios in the Egyptian Mediterranean coast based on six global climate models, *Geofizika Journal, 30*(1), 19-41. UDC 551.581.1, 551.588.7.
- **Shafiei Shiva, J.; Chandler, D. G. and Kunkel, K. E. (2019).** Localized changes in heat wave properties across the United States. *Earth's Future, 7*, 300-319. https://doi.org/10.1029/2018EF001085
- **Tonbol, K.M.; El-Geziry, T.M. and Elbessa, M. (2018).** Evaluation of Changes and Trends of Air Temperature within the Southern Levantine Basin. *Weather, 73*(2): 60-66. DOI: 10.1002/wea.3186.
- **Tuel, A. and Eltahir, E. A. B. (2020).** Why Is the Mediterranean a Climate Change Hot Spot? *Journal of Climate, 33*(14), 5829-5843. https://doi.org/10.1175/JCLI-D-19-0910.1
- **UNESCO (1979).** Map of the world distribution of arid regions (Explanatory note), Published by the United Nations Educational, Scientific and Cultural Organization 7 Place de Fontenoy, 75700 Paris. ISBN 92-3-101484-6, 53pp.COARE and TAO data. *Journal of Climate,11*, 2628-2644.
- **Vigaud, N.; Vrac, M. and Caballero, Y. (2013).** Probabilistic downscaling of GCM scenarios over southern India. *International Journal of Climatology. 33*, 1248-1263. https://doi.org/10.1002/joc.3509
- **Wang, F.; Shao, W.; Yu, H.; Kan, G.; He, X.; Zhang, D.; Ren, M. and Wang, G (2020)**. Re-evaluation of the Power of the Mann-Kendall Test for Detecting Monotonic Trends in Hydrometeorological Time Series. *Frontiers in Earth Science, 8*, 14. https://doi.org/10.3389/feart.2020.00014.
- **Wood A. W.; Maurer E. P.; Kumar A. and Lettenmaier D. P. (2002)**. Longrange experimental hydrologic forecasting for the eastern United States, *Journal of Geophysical Research, 107*(20), 4429, doi:10.1029/2001JD000659.

- **Yadav, R. K. (2021).** Relationship between Azores High and Indian summer monsoon. *Npj Climate and Atmospheric Science, 4*(1). https://doi.org/10.1038/s41612-021-00180-z
- **Zerefos, C.; Repapis, C.; Giannakopoulos, C.; Kapsomenakis, J.; Papanikolaou, D.; Papanikolaou, M.; Poulos, S.; Vrekoussis, M.; Philandras, C.; Tselioudis, G.; Gerasopoulos, E.; Douvis, K.; Diakakis, M.; Nastos, P.; Hadjinicolaou, P.; Xoplaki, E.; Luterbacher, J.; Zanis, P.; Tzedakis, C. and Repapis, K. (2011).** The climate of the Eastern Mediterranean and Greece: past, present, and future. In: The Environmental, Economic and Social Impacts of Climate Change in Greece. Bank of Greece, Athens, pp. 1-126.